Journal of Dental Research
2017, Vol. 96(13) 1518–1525

DOI: 10.1177/0022034517719415
journals.sagepub.com/home/jdr

PAR-1 and PAR-2 Expression Is Enhanced in Inflamed Odontoblast Cells

M.M.P. Alvarez[1], G.E. Moura[1], M.F.M. Machado[2], G.M. Viana[1], C.A. de Souza Costa[3], L. Tjäderhane[4,5], H.B. Nader[1], I.L.S. Tersariol[1], and F.D. Nascimento[2]

Abstract

Protease-activated receptors (PARs) are G protein–coupled receptors, which are activated by proteolytical cleavage of the amino-terminus and act as sensors for extracellular proteases. We hypothesized that PAR-1 and PAR-2 can be modulated by inflammatory stimulus in human dental pulp cells. PAR-1 and PAR-2 gene expression in human pulp tissue and MDPC-23 cells were analyzed by quantitative polymerase chain reaction. Monoclonal PAR-1 and PAR-2 antibodies were used to investigate the cellular expression of these receptors using Western blot, flow cytometry, and confocal microscopy in MDPC-23 cells. Immunofluorescence assays of human intact and carious teeth were performed to assess the presence of PAR-1 and PAR-2 in the dentin-pulp complex. The results show for the first time that human odontoblasts and MDPC-23 cells constitutively express PAR-1 and PAR-2. PAR-2 activation increased significantly the messenger RNA expression of matrix metalloproteinase (MMP)–2, MMP-9, MMP-13, and MMP-14 in MDPC-23 cells ($P < 0.05$), while the expression of these enzymes decreased significantly in the PAR-1 agonist group ($P < 0.05$). The high-performance liquid chromatography and matrix-assisted laser desorption/ionization–time-of-flight mass spectrometry analysis showed the presence of MMP-13 activity cleaving PAR-1 at specific, noncanonical site TLDPRS$^{42}\downarrow$F^{43}LL in human dental pulp tissues. Also, we detected a presence of a trypsin-like activity cleaving PAR-2 at canonical site SKGR$^{20}\downarrow$S^{21}LIGRL in pulp tissues. Confocal microscopy analysis of human dentin-pulp complex showed intense positive staining of PAR-1 and PAR-2 in the odontoblast processes in dentinal tubules of carious teeth compared to intact ones. The present results support the hypothesis of activation of the upregulated PAR-1 and PAR-2 by endogenous proteases abundant during the inflammatory response in dentin-pulp complex.

Keywords: proteinase-activated receptor (PAR), dentin-pulp complex, odontoblasts, caries, proteolytic enzymes, matrix metalloproteinases

Introduction

Proteinase-activated receptors (PARs) are G protein–coupled receptors that undergo irreversible proteolytic activation by proteases. Activation occurs via the proteolytic cleavage at the *N*-terminus exodomains, revealing a new *N*-terminal domain that binds intramolecularly to the receptor to initiate signaling. The activation of PARs promotes coupling to heterotrimeric G proteins and subsequent signal regulatory mechanism at the plasma membrane. Four members of the PAR family (PAR-1 to PAR-4) have been described (Déry et al. 1998).

PAR signaling has been implicated in a wide range of pathophysiological processes, such as inflammation, hemostasis, thrombosis, and embryonic development (Ossovskaya and Bunnett 2004). PARs have been characterized in several cellular subtypes, but nothing is known about the presence of PARs in odontoblasts. In dental tissues, only PAR-2 has been described in neuronal pulp cells associated with the nociceptive TRPV receptors (Henry and Hargreaves 2007), in dental pulp fibroblast-like cells (Lundy et al. 2010), and in periodontal disease (Holzhausen et al. 2005).

The craniofacial skeleton is primarily derived from neural crest–derived mesenchymal cells (Erickson and Reedy 1998). These cells are responsible for building and maintaining the dynamic mineralized tissue complex such as bone and dentin (Narayanan et al. 2001). Odontoblasts secrete dentin organic matrix comparable to that secreted by osteoblasts, which are calcified by hydroxyapatite deposition (Chetty et al. 2016). PAR-1 and PAR-2 are constitutively expressed by osteoblasts, where they are involved in the cellular differentiation and

[1]Department of Biochemistry, Molecular Biology Division, Federal University of São Paulo (UNIFESP), São Paulo, Brazil
[2]Interdisciplinary Center of Biochemistry Investigation (CIIB), University of Mogi das Cruzes, Mogi das Cruzes, Brazil
[3]Department of Physiology and Pathology, Araraquara School of Dentistry, Univ Estadual Paulista–UNESP, São Paulo, Brazil
[4]Department of Oral and Maxillofacial Diseases, University of Helsinki, and Helsinki University Hospital, Helsinki, Finland
[5]Research Unit of Oral Health Sciences and Medical Research Center Oulu (MRC Oulu), Oulu University Hospital and University of Oulu, Oulu, Finland

A supplemental appendix to this article is available online.

Corresponding Authors:
F.D. Nascimento, Interdisciplinary Center of Biochemistry Investigation (CIIB), University of Mogi das Cruzes, Av. Dr. Cândido Xavier de Almeida e Souza, 200 - 1S15, Mogi das Cruzes - SP, 08780-911, Brazil.
Email: fdnascimento@gmail.com
I.L.S. Tersariol, Department of Biochemistry, Molecular Biology Division, Federal University of São Paulo (UNIFESP), Rua três de maio, 100-4th floor, 04044-020, São Paulo, Brazil.
Email: ivarne.tersariol@gmail.com

inflammatory response (Abraham et al. 2000; Song et al. 2005). The activation of PAR-2 in bone marrow contributes also to the differentiation of both the osteoblast and osteoclast lineages regulating skeletal growth and bone repair (Georgy et al. 2012). Furthermore, the activation of PAR-2 inhibits the differentiation of osteoclasts induced by cytokines in bone marrow cultures and may protect against uncontrolled bone resorption during inflammation (Smith et al. 2004).

The odontoblasts are strong candidates to present at least 1 member of the PAR family, since they are the first to meet external inflammatory stimuli, such as infection in dental caries (Kamio et al. 2008; Lundy et al. 2010). Indeed, through inflammatory stimuli, such as lipopolysaccharide (LPS), the odontoblasts can orchestrate the pulpal inflammatory response (Veerayutthwilai et al. 2007; Bleicher 2014) by producing a wide variety of cytokines and chemokines (Staquet et al. 2008) such as tumor necrosis factor (TNF)–α, interleukin (IL)–8, TLR2, and TLR4 in odontoblast cells (Bleicher 2014).

Since PARs are involved in the remodeling process of the extracellular matrix in other mineralized tissues (Smith et al. 2004; Amiable et al. 2009), we hypothesized that PARs can play a role in the human dentin-pulp complex during the inflammatory process. Therefore, we studied the expression profile of 2 PAR family members in human dentin-pulp complex and MDPC-23 odontoblast-like cells. In addition, was also tested if PAR activation can regulate the expression and activity of matrix metalloproteinases (MMPs).

Materials and Methods

The study protocol was approved by the institutional review board (IRB) committee of Mogi das Cruzes University. Samples were collected with patients' informed consent and consisted of 12 molars, 6 intact third molars, and 6 with active caries lesions and irreversible pulpits, which were extracted for therapeutic reasons from individuals aged 25 to 38 y. The pulp tissue from all 12 teeth was removed, washed with phosphate-buffered saline (PBS), and stored at −80°C until messenger RNA (mRNA) extraction. Reagents were purchased from Sigma Chemical unless otherwise specified.

Specimen Preparation

Third molar crowns (from 3 intact and 3 caries-affected teeth) were cut perpendicular to their longitudinal axis with a slow-speed diamond saw under water irrigation (Isomet; Buehler) to produce one 300-µm-thick slice per tooth. The slices were washed with PBS, fixed with 2% formaldehyde for 30 min at room temperature (RT), and demineralized in EDTA 0.1 mol/L for 2 mo. After demineralization, slices were soaked in Tissue-Tek (Sakura). Subsequently, sections of 15 µm of the teeth were cut on the cryostat (Microm HM 550 Cryostat; Thermo Scientific). After cutting, the tissue slices were adhered on previously silanized slides for subsequent immunostaining (Tersariol et al. 2010). (For detailed description, see Appendix.)

Cell Line and Culture Conditions

MDPC-23 cells (Hanks et al. 1998) were seeded in 25-cm^2 plastic flasks using plain Dulbecco's modified Eagle's medium (Sigma-Aldrich) supplemented with 10% fetal bovine serum (GIBCO), containing 100 IU/mL penicillin, 100 µg/mL streptomycin (Sigma-Aldrich), and 2 mmol/L glutamine (Sigma-Aldrich); pH 6.8; HCl 4N. The cells were maintained in an incubator at 37°C with 5% CO_2.

Quantification of Gene Expression

Total RNA from MDPC-23 cells and pulp tissues cells was extracted using the TRIzol reagent, and the reverse-transcribed complementary DNA (cDNA) was obtained using the ImProm-II Reverse Transcriptase System kit (Promega) according to the manufacturer's protocol. Real-time quantitative polymerase chain reaction (qRT-PCR) assays were performed using the SYBR Green PCR Master Mix (Thermo Fisher Scientific). The cycling parameters for the PCRs were 50°C for 2 min and 95°C for 10 min, followed by 40 cycles at 95°C for 15 s and 60°C for 1 min in an ABI PRISM 7500 Real Time PCR System (Applied Biosystems). (For detailed description, see Appendix Table 1 for primer sequences.)

Western Blot Assay

Cell lysates of MDPC-23 cells were prepared using ice-cold lysis buffer containing 1% Nonidet P-40, 0.1% sodium dodecyl sulfate, 0.5% deoxycholic acid, and complete protease inhibitor mixture (Roche Applied Science). Protein concentrations were estimated using the Bio-Rad protein assay kit. Protein lysates were resolved by sodium dodecyl sulfate polyacrylamide gel electrophoresis (SDS-PAGE), and immunoblots were probed with the indicated primary antibody and detected with horseradish peroxidase (HRP)–conjugated secondary antibody using SuperSignal chemiluminescent substrate (Crisp and Dunn 1994) on the ChemDoc MP image system (Bio-Rad). The relative quantification of the protein expression levels (experimental/control) was determined by densitometry of the electrophoretic bands, and the target protein expression was normalized to the housekeeping protein cytochrome c oxidase subunit IV (COX-IV) for MDPC-23 cells. The antibodies, rabbit anti-mouse P44/42 MAPK (ERK 1/2) and Phospho-p44/42 MAPK (Erk1/2), were used to evaluate PAR-1 functionality. Each figure is representative of the results from 3 experiments conducted in duplicate. (For detailed description of used antibodies, see Appendix Table 2.)

Specimen Analysis

The amount and distribution of PARs in the different compartments of pulp-dentin complex (pulp tissue/chamber, predentin, and dentin—up to 400 µm from predentin) were analyzed by inverted confocal laser scanning microscopy (Leica SP8;

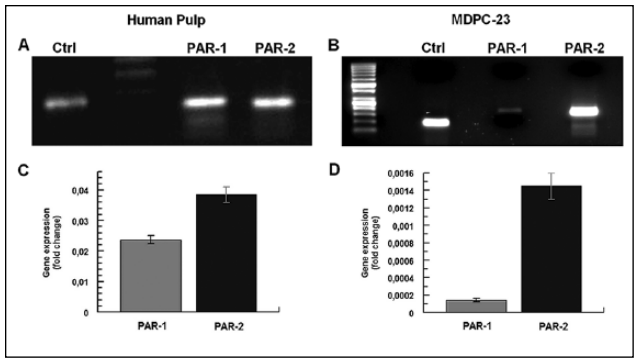

Figure 1. Polymerase chain reaction (PCR) amplification (**A, B**) and real-time quantitative PCR (qRT-PCR) (**C, D**) analysis of expression of protease-activated receptors (PARs) by human pulp cells (A and C) and odontoblast-like MDPC-23 cells (B and D). (A) Lane 1 (left to right): Ctrl, GAPDH primers, and pulp cell RNA; lane 2: RNA molecular weight markers; lane 3: PAR-1 primers and human pulp cell RNA; lane 4: PAR-2 primers and human pulp cell RNA. (B) Lane 1 (left to right): RNA molecular weight markers; lane 2: Ctrl, β-2-microglobulin primers, and MDPC-23 cell RNA; lane 3: PAR-1 primers and MDPC-23 cell RNA; lane 4: PAR-2 primers and MDPC-23 cell RNA. (C–D) The qRT-PCR analysis of PAR-1 and PAR-2 messenger RNA expressions was normalized to the housekeeping gene enzyme GAPDH for human pulp cells (C) and β-2-microglobulin for MDPC-23 cells (D); the relative quantification of the expression levels (experimental/control) was determined based on the 2-[Δ]Ct method as described previously.

Leica). Immunolabeled receptors were observed with a HeNe2 laser with excitation at 633 nm, and fluorescence emission was detected at 640 to 670 nm. Dentin slices were also imaged by differential interference contrast microscopy (DIC) with a HeNe2 laser at 633 nm. False-color fluorescent images and transmitted light images (512 × 512 pixels) were stored, quantified, and managed with resident LAS X software (Leica).

Cellular Localization of the PARs by Confocal Microscopy

For analysis of expression pattern and cellular localization of the PARs through confocal microscopy, MDPC-23 cells were seeded (10^4 cells) onto coverslips until reaching ~70% confluence. Initially, to examine receptor expression at the cell surface, the cells were washed 3 times with PBS, incubated with respective antibodies (mouse anti-human PAR-1 [Millipore] and mouse anti-human PAR-2 [Millipore]), and diluted in PBS at 1:100. Thereafter, cells were incubated with the respective secondary antibody conjugated to Alexa Fluor 488 (Invitrogen). The cells were then fixed with 2% paraformaldehyde/PBS for 30 min, washed 3 times with 0.1 M glycine/PBS, permeabilized with 0.01% saponin/PBS for 15 min, and stained with DAPI for 10 min. The coverslips were mounted onto microscope slides using Fluoromont G (Immunkemi). Light microscopy analysis was performed using a confocal laser-scanning Leica SP8 microscope (Leica). The pinhole device was adjusted to capture the fluorescence of 1 Airy unit. The images were processed using resident LAS X software (Leica).

Measurement of Cytoplasmic Ca^{2+}

MDPC-23 cells were seeded onto black 96-well plates (104 cells/well) and maintained for 48 h at 37°C under an atmosphere of 5% (v/v) CO_2. Subsequently, the cells were incubated with Fluo-4 Direct Calcium Assay (Invitrogen) reagent for 1 h at 37°C, as suggested by manufacturer's instructions. For cytoplasmic Ca^{2+} concentration measurements, the cell samples were stimulated with thrombin, an agonist of PAR-1, or with PAR-2 agonists trypsin and SLIGRL peptide. The resulting fluorescence was measured using a Flex Station 3 microplate reader (Molecular Devices). The Fluo-4 was excited at 490 nm and the emission was detected at 525 nm (Moura et al. 2015).

Flow Cytometry Analysis

PAR expression was determined using flow cytometry analysis. Initially, to examine receptor expression at the cell surface, the cells were incubated with mouse anti-PARs 1 and 2 primary antibodies, washed with PBS buffer, and labeled with the respective secondary antibody conjugated to Alexa Fluor 488. The data were collected using a FACSCalibur flow cytometer (Becton-Dickinson) and CellQuest software (Becton-Dickinson), followed by analysis using FlowJo software (Tree Star). (For detailed description of the flow cytometer assay, see the Appendix.)

Chemical Synthesis of Fluorescence Resonance Energy Transfer–Peptide

The fluorescence resonance energy transfer (FRET)–peptide substrates containing ortho-aminobenzoic acid (Abz) as the donor group and N-2,4-dinitrophenyl (Dnp) as the acceptor group, Abz-TLDPRSFLLK(Dnp)-NH2 and Abz-SSKGRSLIGK(Dnp)-NH2, were synthesized in solid-phase chemistry (Nunes et al. 2011). The molecular weight and purity of synthesized peptides were checked by matrix-assisted laser desorption/ionization–time-of-flight (MALDI-TOF) mass spectrometry (TofSpec-E; Micromass) and/or peptide sequencing using a protein sequencer PPSQ-23 (Shimadzu). (For detailed description of FRET-peptide synthesis, see the Appendix.)

Enzyme Activities

The endopeptidase activities present in the homogenate of pulp tissues were monitored fluorometrically using the FRET substrates that mimic the primary sequences of PAR-1 and PAR-2 at cleavage sites Abz-TLDPRSFLLK(Dnp)-NH2 and Abz-SSKGRSLIGK(Dnp)-NH2, respectively (Nunes et al. 2011). The fluorescence intensity was monitored on a thermostatic Hitachi F-2500 spectrofluorimeter. (For detailed description of enzyme activity assay, see the Appendix.)

Statistical Analysis

Statistical analysis was performed using GraphPad Prism 5.0 software (GraphPad Software). Analysis of variance (ANOVA)

was used to verify the occurrence of significant differences between the studied groups, followed by Bonferroni correction in the posttest. The unpaired 2-tailed Student's *t* test ($P < 0.05$) was applied to test for significant differences between the 2 groups.

Results

The expression of PAR-1 and PAR-2 by human dental pulp cells and by MDPC-23 odontoblast-like cells was investigated by PCR/qRT-PCR, Western blotting, flow cytometry, and immunocytochemistry. PAR-1 and PAR-2 primers detected a major band of the appropriate size mRNA extracted from human dental pulp cells (Fig. 1A), as well as from MDPC-23 cells (Fig. 1B). Intron-spanning PAR-1 and PAR-2 primers detected the predicted size (105 pb) for the appropriate regions of mRNA, indicating the lack of detectable contamination of MDPC-23 cell RNA by genomic DNA (Fig. 1B). Similar results were observed for the RNA extracted from human dental pulp cells (Fig. 1A). The expression level of PAR-1 and PAR-2 mRNAs in human dental pulp cells and MDPC-23 cells was also measured. PAR-2 mRNA expression was 1.7-fold and 8.2-fold higher than PAR-1 expression in human dental pulp cells (Fig. 1C) and in MDPC-23 cells (Fig. 1D), respectively.

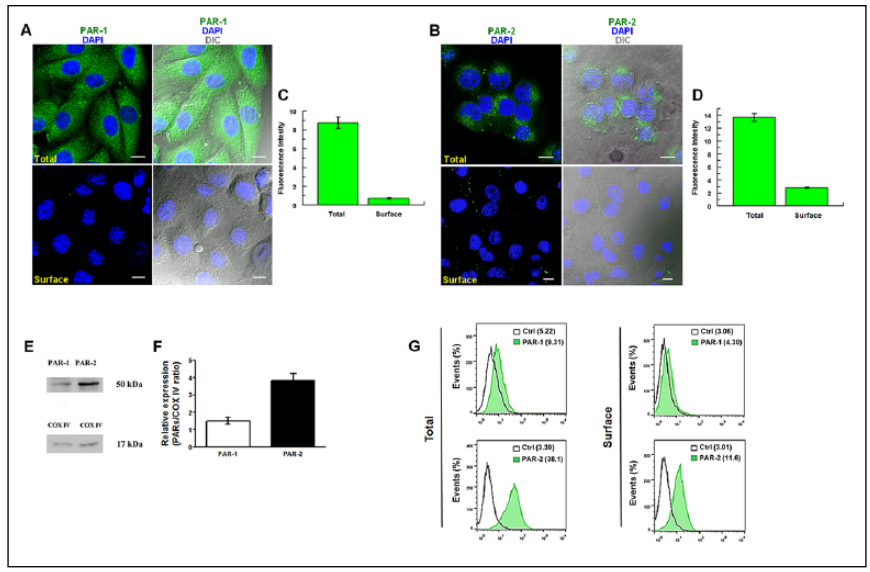

Figure 2. Protease-activated receptor (PAR)–1 and PAR-2 are expressed on the cell surface and in the intracellular compartment of the MDPC-23 cells. (**A**) Confocal laser-scanning microscopic analysis of MDPC-23 cells stained with anti–PAR-1 monoclonal antibody (green), DAPI (4',6-diamidino-2-phenylindole) (blue), and differential interference contrast (DIC) with permeabilization of the membranes (upper panels) and without permeabilization (lower panels). (**B**) Confocal laser-scanning microscopic analysis of MDPC-23 cells stained with anti–PAR-2 monoclonal antibody (green) and DAPI (blue) with permeabilization of the membranes (upper panels) and without permeabilization (lower panels). (**C**) PAR-1 and (**D**) PAR-2 relative fluorescence intensity in MDPC-23 cells. (**E**) Western blotting analysis of whole MDPC-23 cell lysates reveled with anti–PAR-1 monoclonal antibody and with anti–PAR-2 monoclonal antibody (upper panel). Figures are representative of 3 separate experiments. (**F**) Relative arbitrary densitometric units (mean ± SE) obtained from 50-kDa bands of PAR-1 and PAR-2. The relative quantification of the PAR-1 and PAR-2 expression levels (experimental/control) was normalized to the housekeeping COX-IV (17 kDa). (**G**) Flow cytometric analysis of MDPC-23 cells stained with anti–PAR-1 monoclonal antibody (upper panels) or anti–PAR-2 monoclonal antibody (lower panels) before (right panels) and after (left panels) membrane permeabilization with saponin.

Monoclonal antibodies against PAR-1 and PAR-2 were used to investigate the cellular receptor expression and localization in MDPC-23 cells using confocal microscopy (Fig. 2A, B). Eight percent of PAR-1 receptors (Fig. 2C) and 23% of PAR-2 receptors (Fig. 2D) were localized on the MDPC-23 cell surface. Western blot analysis (Fig. 2E, F) of the MDPC-23 cell homogenates shows the expression of the 50-kDa forms of PAR-1 and PAR-2 receptors (Canto and Trejo 2013). The quantification of PAR-1 and PAR-2 receptor expression through flow cytometry analysis also revealed that PAR-2 is 8.5-fold more expressed in MDPC-23 cells than PAR-1 (Fig. 2G), corroborating the qRT-PCR data described in Figure 1.

The functionality of PAR-1 and PAR-2 receptors was verified by the cellular response of these receptors through stimulation with their classical agonists (Fig. 3A, B). Interestingly, stimulation of PAR-1 with thrombin, the natural PAR-1 activator, did not promote influx of Ca^{2+} into MDPC-23 cytoplasm (Fig. 3A) but induced phosphorylation of ERK 1/2 in a time-dependent manner (Fig. 3B–D). However, trypsin (Fig. 3E) and the specific peptide activator of PAR-2 SLIGRL (Fig. 3F) induced a dose-dependent transient Ca^{2+} cytoplasmic influx.

The expression of both PAR-1 and PAR-2 mRNA was significantly increased in pulp tissue with acute irreversible pulpitis compared to the healthy pulp (Fig. 4A). Pretreatment of MDPC-23 cells with LPS (100 ng/mL) significantly increased the gene expression of the PAR-1 (5-fold) and PAR-2 (70-fold) (Fig. 4B). An increase in the TNF-α and IL-6 gene expression occurred in the presence of LPS, as expected (Fig. 4B). PAR-1 activation promoted a significant inhibition in MMP-2, MMP-13, and MMP-14 gene expression, while the expression of MMP-9 was not significantly altered (Fig. 4C). On the other hand, the stimulation of PAR-2 promoted a significant increase in the gene expression of MMP-2, MMP-9, MMP-13, and MMP-14 (Fig. 4D). Interestingly, the nuclear factor (NF)–κB gene expression was significantly decreased, whereas a large increase in TNF-α expression was observed after activation of PAR-1 or PAR-2 (Fig. 4C, D).

The mechanism of PAR-1 and PAR-2 activation by proteolytic enzymes in normal and inflamed human pulp tissue was evaluated using FRET-peptides. The sequences Abz-TLDPR SFLLK(Dnp)-NH2 and Abz-SSKGRSLIGK(Dnp)-NH2, which mimic the primary domain of PAR-1 between residues 37 and 46 and PAR-2 between residues 15 and 24 at the cleavage sites, respectively, were assayed. As expected, markedly higher

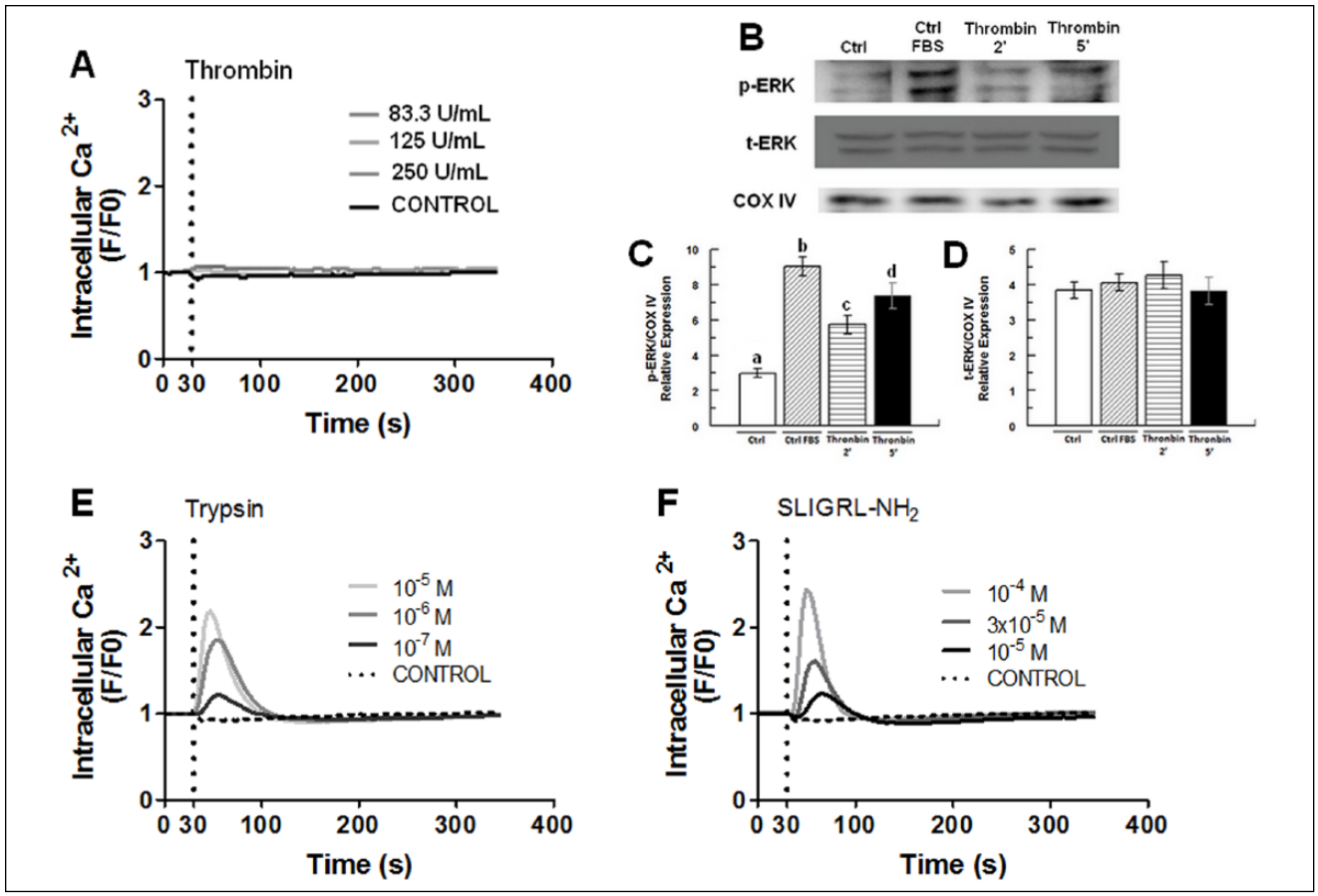

Figure 3. Intracellular responses elicited by protease-activated receptor (PAR)–1 and PAR-2 activation. (**A**) Intracellular calcium mobilization in Fluo-4–loaded MDPC-23 cells treated with different concentrations of thrombin, demonstrating no calcium influx by PAR-1 activation. (**B**) ERK1/2 phosphorylation was observed after treatment of MDPC-23 cells with thrombin (10 U/mL) for the indicated times (2 or 5 min), 10% fetal bovine serum (FBS) for 5 min, or untreated. Whole-cell lysates were immunoblotted and probed for phospho-ERK1/2 and total-ERK1/2. (**C, D**) Mean ± SE relative arbitrary densitometric units obtained from phospho-ERK1/2 (C) and total ERK1/2 (D); the relative quantification of the phospho-ERK1/2 and total-ERK1/2 expression levels (experimental/control) was normalized to the housekeeping protein COX-IV. Blots are representative of 3 independent experiments (mean ± SEM). (a) Ctrl, control phospho-ERK1/2 (3.0 ± 0.2 DU); (b) 10% SBF (9.2 ± 0.8 DU), $P = 0.001$; (c) thrombin 2 min (5.6 ± 0.5 DU), $P = 0.0074$; (d) thrombin 5 min (7.5 ± 0.6 DU), $P = 0.0019$. (**E**) Trypsin and (**F**) rat PAR-2 agonist peptide SLIGRL, as indicated on individual traces, demonstrating transient concentration-dependent calcium influx due to PAR-2 activation.

proteolytic activities against both peptides were observed in inflamed pulp than in normal pulp (Fig. 4E). The HPLC and MALDI-TOF mass spectrometry analysis showed that S^{42}-F^{43} was the only peptide bond cleaved by an MMP on the mimetic peptide of PAR-1, Abz-TLDPRS↓FLLK (Dnp)-NH2 (Fig. 4F). The mimetic substrate of PAR-2 was cleaved by a serine protease at R^{20}-S^{21} and by an MMP at G^{19}-R^{20}, Abz-SSKG↓R↓SLIGK (Dnp)-NH2 (Fig. 4G). The pretreatment of the sample with phenylmethylsulfonyl fluoride (PMSF) abolished the peptide hydrolysis at R^{20}-S^{21}, and the pretreatment with 1,10 phenanthroline abolished the substrate cleavage at G^{19}-R^{20}.

Human dental-pulp complex also constitutively expressed PAR-1 and PAR-2 in the odontoblastic region (Fig. 5). In intact dentin, immunostaining of the dental-pulp complex region showed that labeling was 1.9-fold more intensive for PAR-2 compared to PAR-1 (Fig. 5A, B). Using human dental caries as a model, we studied the influence of the in vivo inflammatory process on the gene expression of PAR-1 and PAR-2. The predentin-dentin morphology for intact and caries-affected dentin can be observed by differential interference contrast (DIC) (Fig. 5A, B, panels a and d). PAR-1 and PAR-2 were detected and stained in red at the odontoblast-predentin region (Fig. 5A, B, panels c and f). Immunodetection of the PAR-1 and PAR-2 was markedly higher in the odontoblast cell layer and in the odontoblast processes of carious teeth compared to the healthy teeth (Fig. 5A, B and Fig. 5C, D).

Discussion

The present study shows for the first time that human odontoblasts and MDPC-23 odontoblast-like cells constitutively express PAR-1 and PAR-2. The PAR-2 gene expression was significantly higher than PAR-1 expression both in human tissues and in MDPC-23 cells. Both cell surface and intracellular PAR-1 and PAR-2 were detected in the MDPC-23 cells.

PAR-2 activators trypsin and SLIGRL peptide initiated a dose-dependent transient Ca^{2+} influx into MDPC-23 cytoplasm similar to that observed with the rat calvarial osteoblast-like cells (Abraham et al. 2000). However, stimulation of MDPC-23 cells with PAR-1 activator thrombin resulted in phosphorylation of the ERK 1/2 in a time-dependent manner. The activation of ERK 1/2 by phosphorylation is involved in the process of cellular differentiation of odontoblast-like MDPC-23 cells (Yao et al. 2011; Sagomonyants et al. 2015). Our results confirm the presence of functional PAR-1 and PAR-2 and indicate differential regulatory mechanisms on MDPC-23 odontoblast-like cells.

We also showed that LPS promotes a considerable increase in the PAR-1 and PAR-2 gene expression in MDPC-23 cells, accompanied by increased expression of the TNF-α and IL-6 genes, suggesting that these receptors may be involved in the inflammatory response triggered by LPS. The inflammatory process induced by caries in the stem cells present in the pulp tissue can induce differentiation of odontoblast-like cells and favor the process of dentin mineralization by decreasing the gene expression of NF-κB (Hozhabri et al. 2015); elevation in the expression of NF-κB inhibits the process of odontoblast differentiation (Pei et al. 2016). Amiable et al. (2009) showed that PAR-2 expression is significantly increased in the presence of TNF-α in osteoblasts. Together these data suggest the cooperation between the PARs, LPS receptors, and TNF-α in the amplification of the inflammatory signal in odontoblasts, which in turn can induce the process of cellular differentiation.

The increase in PAR-1 and PAR-2 expression triggered by an inflammatory stimulus was also observed in vivo in histological sections of human carious teeth. We observed an intense and increased positive labeling with the anti–PAR-1 and anti–PAR-2 monoclonal antibodies in the odontoblasts, indicating that the inflammatory process triggered by bacterial infection promoted a large increase in PAR-1 and PAR-2 expression. Also, it is important to mention that in the carious teeth, PAR-1 and PAR-2 receptors were present mostly in the odontoblast processes embedded into dentinal tubules, whereas in healthy teeth, the PAR-1 and PAR-2 receptors were mostly present in the cell bodies.

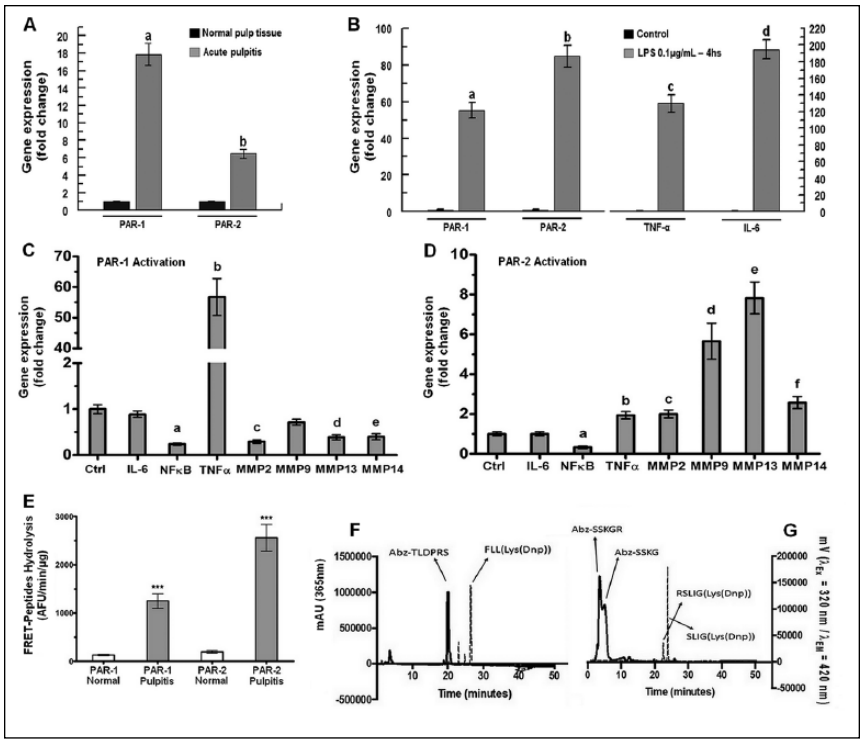

Figure 4. Inflammatory stimulus enhances protease-activated receptor (PAR)–1 and PAR-2 messenger RNA (mRNA) expression and activation of the by PAR-1 and PAR-2 endogenous proteases in human pulp tissue and MDPC-23 cells. (**A**) Real-time quantitative polymerase chain reaction (qRT-PCR) analysis of PAR-1 and PAR-2 mRNA expression in pulp tissue from healthy and carious teeth with acute irreversible pulpitis (n = 6/group). The qRT-PCR analysis of the target mRNA expression was normalized to the housekeeping gene enzyme GAPDH for human pulp cells and further to the values of healthy pulp tissue (level = 1). (**B**) MDPC-23 cells treated or not with lipopolysaccharide (LPS) 0.1 µg/mL for 4 h. The bars represent the gene expression levels of PAR-1, PAR-2, tumor necrosis factor (TNF)–α and interleukin (IL)–6 mRNA after LPS treatment, which was normalized to the level of untreated cells (mean ± SEM). The qRT-PCR analysis of the target mRNA expression was normalized to the housekeeping gene β-2-microglobulin for MDPC-23 cells and further to the values of untreated MDPC-23 cells (level = 1). The relative quantification of the expression levels (experimental/control) in both A and B was determined based on the 2-[Δ]Ct method as previously described. All experiments were performed in triplicate. Lowercase letters indicate statistically significant differences (P < 0.0001). (**C**) MDPC-23 cells treated or not with 100 µM peptide agonist of PAR-1, TFLLR-NH2, for 2 h. The bars represent the mRNA expression levels of IL-6, nuclear factor (NF)–κB, TNF-α, matrix metalloproteinase (MMP)–2, MMP-9, and MMP-14 after TFLLR-NH2 treatment, which was normalized to the level of untreated cells (mean ± SEM, n = 6). Lowercase letters indicate statistically significant differences (P < 0.05). (**D**) MDPC-23 cells treated or not with 100 µM peptide agonist of PAR-2, SLIGPRL-NH2, for 2 h. The bars represent the mRNA expression levels of IL-6, NF-κB, TNF-α, MMP-2, MMP-9, and MMP-14 after SLIGRL-NH2 treatment, which was normalized to the level of untreated cells (mean ± SEM, n = 6). Lowercase letters indicate statistically significant differences (P < 0.05). (**E**) Specific activity of hydrolysis on the mimetic fluorescence resonance energy transfer (FRET)–peptide of PAR-1, Abz-TLDPRSFLLK(Dnp)-NH2, and PAR-2, Abz-SSKGRSLIGK(Dnp)-NH2. The bars represent the specific activity of hydrolysis (AFU/min/µg) by proteinases present in pulp tissues on the mimetic FRET-peptides (mean ± SEM, n = 3). (**F, G**) Determination of proteinase cleavage site by high-performance liquid chromatography (HPLC) and matrix-assisted laser desorption/ionization–time-of-flight (MALDI-TOF) mass spectrometry. (F) PAR-1 mimetic FRET-peptide, Abz-TLDPRSFLLK(Dnp)-NH2, and (G) PAR-2 mimetic, FRET-peptide, AbzSSKGRSLIGK(Dnp)-NH2. The enzymatic products of these incubations were analyzed using a binary HPLC. The molecular weight and purity of synthesized peptides and enzymatic products were checked by MALDI-TOF mass spectrometry.

We have previously shown high expression of cysteine cathepsins and MMPs in carious dentin, indicating that those host-derived proteases are intensely involved with caries progression (Nascimento et al. 2011; Vidal et al. 2014). PAR-2 activating peptide significantly increased the expressions of MMP-2, MMP-9, MMP-13, and MMP-14 in MDPC-23 cells.

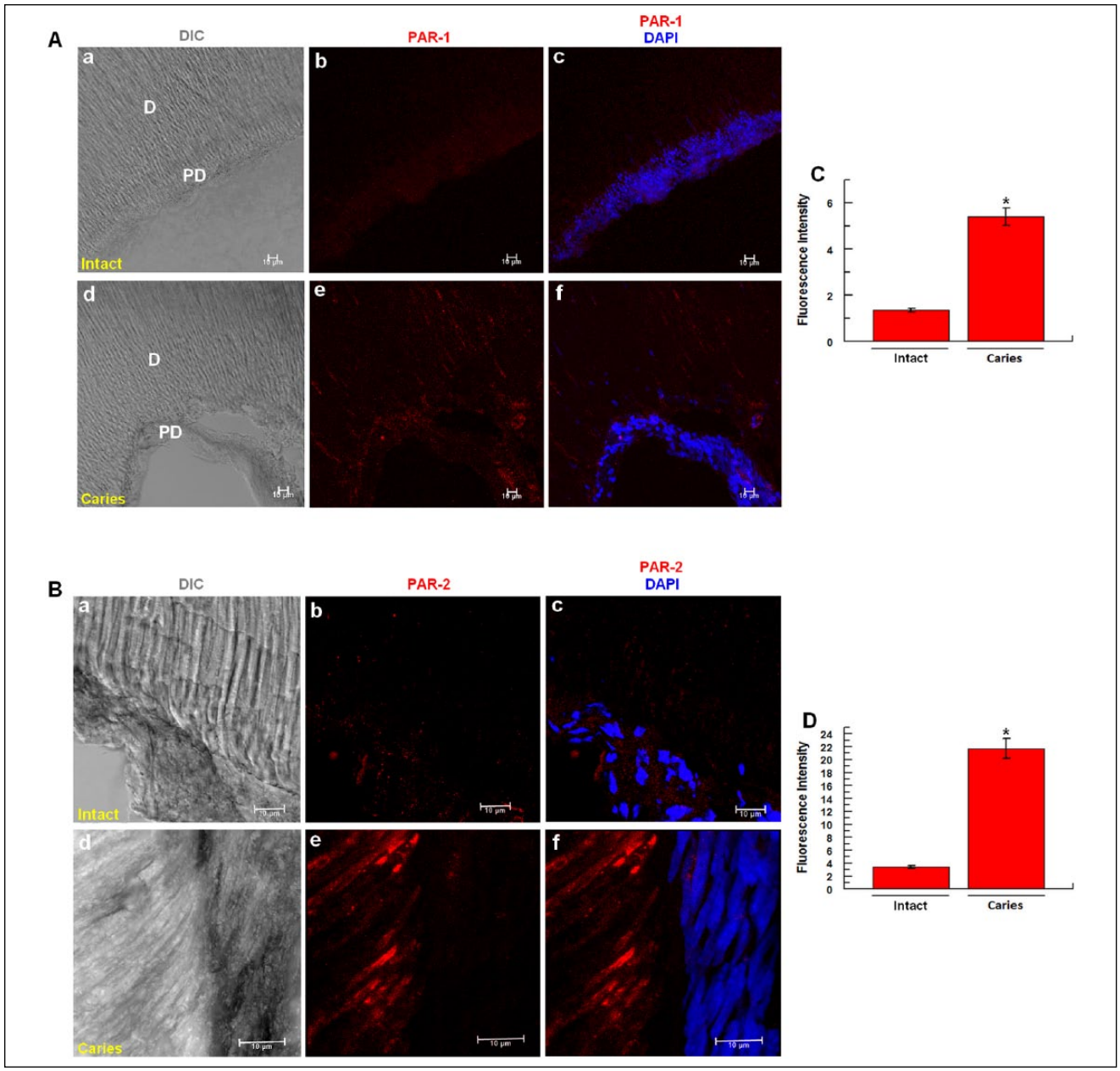

Figure 5. Immunohistochemistry detection of the protease-activated receptor (PAR)–1 (**A**, **C**) and PAR-2 (**B**, **D**) in intact and carious teeth by confocal microscopy. Intact and caries-affected dentin morphology observed in differential interference contrast (DIC) mode (Aa, Ad, Ba, and Bd). (A) PAR-1 immunolabeling shown in the red channel in intact (Ab) and caries-affected (Ae) dentin (Ac and Af). Merged images of PAR-1 and in the blue nuclear odontoblastic region (DAPI) in intact (Ac) and caries-affected (Af) dentin. (B) PAR-2 immunolabeling shown in the red channel in intact (Bb) and caries-affected (Be) dentin. Merged images of PAR-1 and odontoblastic region (Bc and Bf). (C–D) Quantification of emitted fluorescence, PAR-1 (C) and PAR-2 (D) relative fluorescence intensity, in intact and caries-affected dentin. All experiments were performed in triplicate. *$P < 0.05$. D, dentin; PD, predentin.

On the other hand, the activation of PAR-1 significantly decreased the expression of MMP-2, MMP-13, and MMP-14.

It is worth mentioning that at least MMP-1 and MMP-13 hydrolyze and activate PAR-1 at a noncanonical domain (Austin et al. 2013) and are both expressed by human odontoblasts (Palosaari et al. 2003). In sound dentin, MMP-13 is weakly expressed and confined to the peritubular area, but in caries-affected dentin, the expression is increased not only at the peritubular level but also at the odontoblast processes region (Loreto et al. 2014). The cleavage of PAR-1 at a specific, noncanonical extracellular site TLDPRS$^{42}\downarrow$F^{43}LL by MMP-13 generates a tethered ligand F^{43}LLRN that, in turn, activates PAR-1 differently from that produced by thrombin (Austin et al. 2013). Therefore, the observed enzymatic

cleavage of mimetic FRET-peptide of PAR-1 at a specific, non-canonical extracellular site TLDPRS^{42}↓F^{43}LL may be attributed to the presence of MMP-13 activity in pulp tissue.

Trypsin-like proteases hydrolyze PAR-2 at SKGR^{20}↓S^{21}LIGRL to generate the S^{21}LIGRL-tethered ligand that activates PAR-2 (Rothmeier and Ruf 2012). We also observed a typical trypsin-like proteinase cleaving the mimetic peptide of PAR-2 at a canonical extracellular site at NSKGR^{20}↓S^{21}LIG. Taken together, these data suggest that PAR-1 and PAR-2 are orchestrating the proteolytic balance in dental pulp tissue.

The present results support the hypothesis of activation of upregulated PAR-1 and PAR-2 by endogenous proteases abundant during the inflammatory response in dentin-pulp complex. Therefore, the possible role of protease-activated PAR-1 and PAR-2 in the odontoblasts and in dental pulp cells may be related to physiological secondary dentine formation and mineralization in intact teeth, matrix degradation during dental injury, regulation of reactionary/reparative dentinogenesis, and regulation of pulp inflammation.

Author Contributions

M.M.P. Alvarez, contributed to data acquisition and analysis; G.E. Moura, contributed to data acquisition, interpretation, drafted and critically revised the manuscript; M.F.M. Machado, contributed with the enzyme kinetic assays. G.M. Viana, contributed to confocal microscopy image acquisition, quantification and interpretation; C.A. de Souza Costa, contributed to data interpretation and critically revised the manuscript; L. Tjaderhane, H.B. Nader, contributed to data interpretation, drafted and critically revised the manuscript; I.L.S. Tersariol and F.D. Nascimentos, contributed to conception, design, data acquisition, analysis, and interpretation, drafted and critically revised the manuscript. All authors gave final approval and agree to be accountable for all aspects of the work.

Acknowledgments

We thank the following funding agencies: FAPESP (grants 13/05822-9 and 15/03964-6), CAPES, and CNPq, Brazil. The authors declare no potential conflicts of interest with respect to the authorship and/or publication of this article.

References

Abraham LA, Chinni C, Jenkins AL, Lourbakos A, Ally N, Pike RN, Mackie EJ. 2000. Expression of protease-activated receptor-2 by osteoblasts. Bone. 26(1):7–14.

Amiable N, Tat SK, Lajeunesse D, Duval N, Pelletier JP, Martel-Pelletier J, Boileau C. 2009. Proteinase-activated receptor (PAR)-2 activation impacts bone resorptive properties of human osteoarthritic subchondral bone osteoblasts. Bone. 44(6):1143–1150.

Austin KM, Covic L, Kuliopulos A. 2013. Matrix metalloproteases and par1 activation. Blood. 121(3):431–439.

Bleicher F. 2014. Odontoblast physiology. Exp Cell Res. 325(2):65–71.

Canto I, Trejo J. 2013. Palmitoylation of protease-activated receptor-1 regulates adaptor protein complex-2 and -3 interaction with tyrosine-based motifs and endocytic sorting. J Biol Chem. 288(22):15900–15912.

Chetty M, Roberts T, Stephen LX, Beighton P. 2016. Hereditary dentine dysplasias: terminology in the context of osteogenesis imperfecta. Br Dent J. 221(11):727–730.

Crisp SJ, Dunn MJ. 1994. Detection of proteins on protein blots using chemiluminescent systems. Methods Mol Biol. 32:233–237.

Déry O, Corvera CU, Steinhoff M, Bunnett NW. 1998. Proteinase-activated receptors: novel mechanisms of signaling by serine proteases. Am J Physiol. 274(6 Pt 1):C1429–C1452.

Erickson CA, Reedy MV. 1998. Neural crest development: the interplay between morphogenesis and cell differentiation. Curr Top Dev Biol. 40:177–209.

Georgy SR, Pagel CN, Ghasem-Zadeh A, Zebaze RM, Pike RN, Sims NA, Mackie EJ. 2012. Proteinase-activated receptor-2 is required for normal osteoblast and osteoclast differentiation during skeletal growth and repair. Bone. 50(3):704–712.

Hanks CT, Sun ZL, Fang DN, Edwards CA, Wataha JC, Ritchie HH, Butler WT. 1998. Cloned 3T6 cell line from CD-1 mouse fetal molar dental papillae. Connect Tissue Res. 37(3–4):233–249.

Henry MA, Hargreaves KM. 2007. Peripheral mechanisms of odontogenic pain. Dent Clin N Am. 51(1):19–44.

Holzhausen M, Spolidorio LC, Vergnolle N. 2005. Proteinase-activated receptor-2 (PAR2) agonist causes periodontitis in rats. J Dent Res. 84(2):154–159.

Hozhabri NS, Benson MD, Vu MD, Patel RH, Martinez RM, Nakhaie FN, Kim HK, Varanasi VG. 2015. Decreasing NF-κB expression enhances odontoblastic differentiation and collagen expression in dental pulp stem cells exposed to inflammatory cytokines. PLoS One. 10(1):e0113334.

Kamio N, Hashizume H, Nakao S, Matsushima K, Sugiya H. 2008. Plasmin is involved in inflammation via protease-activated receptor-1 activation in human dental pulp. Biochem Pharmacol. 75(10):1974–1980.

Loreto C, Galanti C, Musumeci G, Rusu MC, Leonardi R. 2014. Immunohistochemical analysis of matrix metalloproteinase-13 in human caries dentin. Eur J Histochem. 58(1):2318.

Lundy FT, About I, Curtis TM, McGahon MK, Linden GJ, Irwin CR, El Karim IA. 2010. Par-2 regulates dental pulp inflammation associated with caries. J Dent Res. 89(7):684–688.

Moura G, Lucena SV, Lima MA, Nascimento FD, Gesteira TF, Nader HB, Paredes-Gamero EJ, Tersariol I. 2015. Post-translational allosteric activation of the P2X7 receptor through glycosaminoglycan chains of CD44 proteoglycans. Cell Death Discov. 1:15005.

Narayanan K, Srinivas R, Ramachandran A, Hao J, Quinn B, George A. 2001. Differentiation of embryonic mesenchymal cells to odontoblast-like cells by overexpression of dentin matrix protein 1. Proc Natl Acad Sci USA. 98(8):4516–4521.

Nascimento FD, Minciotti CL, Geraldeli S, Carrilho MR, Pashley DH, Tay FR, Nader HB, Salo T, Tjaderhane L, Tersariol IL. 2011. Cysteine cathepsins in human carious dentin. J Dent Res. 90(4):506–511.

Nunes GL, Simoes A, Dyszy FH, Shida CS, Juliano MA, Juliano L, Gesteira TF, Nader HB, Murphy G, Chaffotte AF, et al. 2011. Mechanism of heparin acceleration of tissue inhibitor of metalloproteases-1 (TIMP-1) degradation by the human neutrophil elastase. PLoS One. 6(6):e21525.

Ossovskaya VS, Bunnett NW. 2004. Protease-activated receptors: contribution to physiology and disease. Physiol Rev. 84(2):579–621.

Palosaari H, Pennington CJ, Larmas M, Edwards DR, Tjaderhane L, Salo T. 2003. Expression profile of matrix metalloproteinases (MMPs) and tissue inhibitors of MMPs in mature human odontoblasts and pulp tissue. Eur J Oral Sci. 111(2):117–127.

Pei F, Wang HS, Chen Z, Zhang L. 2016. Autophagy regulates odontoblast differentiation by suppressing NF-κB activation in an inflammatory environment. Cell Death Dis. 7:e2122.

Rothmeier AS, Ruf W. 2012. Protease-activated receptor 2 signaling in inflammation. Semin Immunopathol. 34(1):133–149.

Sagomonyants K, Kalajzic I, Maye P, Mina M. 2015. Enhanced dentinogenesis of pulp progenitors by early exposure to FGF2. J Dent Res. 94(11):1582–1590.

Smith R, Ransjo M, Tatarczuch L, Song SJ, Pagel C, Morrison JR, Pike RN, Mackie EJ. 2004. Activation of protease-activated receptor-2 leads to inhibition of osteoclast differentiation. J Bone Miner Res. 19(3):507–516.

Song SJ, Pagel CN, Pike RN, Mackie EJ. 2005. Studies on the receptors mediating responses of osteoblasts to thrombin. Int J Biochem Cell Biol. 37(1):206–213.

Staquet MJ, Durand SH, Colomb E, Romeas A, Vincent C, Bleicher F, Lebecque S, Farges JC. 2008. Different roles of odontoblasts and fibroblasts in immunity. J Dent Res. 87(3):256–261.

Tersariol IL, Geraldeli S, Minciotti CL, Nascimento FD, Paakkonen V, Martins MT, Carrilho MR, Pashley DH, Tay FR, Salo T, et al. 2010. Cysteine cathepsins in human dentin-pulp complex. J Endod. 36(3):475–481.

Veerayutthwilai O, Byers MR, Pham TT, Darveau RP, Dale BA. 2007. Differential regulation of immune responses by odontoblasts. Oral Microbiol Immunol. 22(1):5–13.

Vidal CM, Tjaderhane L, Scaffa PM, Tersariol IL, Pashley D, Nader HB, Nascimento FD, Carrilho MR. 2014. Abundance of MMPs and cysteine cathepsins in caries-affected dentin. J Dent Res. 93(3):269–274.

Yao N, Li S, Jiang Y, Qiu S, Tan Y. 2011. Amelogenin promotes odontoblast-like MDPC-23 cell differentiation via activation of ERK1/2 and p38 MAPK. Mol Cell Biochem. 355(1–2):91–97.